Development of beneficiation circuit for low-grade laterite iron ores sourced from the Gujarat area

Byra Reddy Raghunatha Reddy[1*], Vardhan Harsha[1], Arya Shashi Bhushan[2], Hanumanthappa Harish[3] and Shanmugam Bharath Kumar[4]

1. Dept. of Mining Engineering, National Institute of Technology Karnataka, Mangalore, Karnataka, 575025, INDIA
2. Dept. of Metallurgical and Materials Engineering, National Institute of Technology Karnataka, Mangalore, Karnataka, 575025, INDIA
3. RV University, RV Vidyanikethan Post, 8th Mile, Mysore Rd, Mailasandra, Bengaluru, Karnataka, 560059, INDIA
4. Dept. of AI and Robotics. Engg., Dayananda Sagar University (DSU), Main Campus, Ramanagara Dt, Karnataka, 562112, INDIA
*raghu.bkbreddy@gmail.com

Abstract

This study focuses on the maximum recovery of iron values from the low-grade laterite iron ore. The Fe analysis of laterite was carried out using wet method analysis. Subsequently, the characterization studies were carried out on laterite ore using Optical microscope for liberation studies, mineral phase analysis with XRD and elemental analysis using SEM-EDS. Further, the ore of feed particle size of -150 microns was subjected to physical separation techniques such as scrubbing, hydro cyclone, spiral concentrator and dual-stage HGMS and two beneficiation circuits.

The results from the above physical separation beneficiation techniques showed a concentrate of 41.25% Fe_G and a recovery of 48.05% in beneficiation circuit 1 and a concentrate of 48.03 % Fe_G and a recovery of 62.11% in beneficiation circuit 2 which is not feasible for iron-making in the blast furnace.

Keywords: Laterite iron ore, particle size distribution, scrubber, spiral concentrator, hydrocyclone, dual-stage HGMS, magnetic separator.

Introduction

The quality of iron ore is crucial for the production of iron and steel. India lacks high-grade iron ores but has abundant low-grade iron ores like laterite iron ores to meet the 300 million steel production target of the Steel Policy 2030[6,8,13,14]. The laterite ores are seasoned ores and this ore suffered significant laterization effects associated with high silica and alumina.

Generally, the LGIO lumps are of two types: type I: Partially laterized lumps, iron rich hard ore with hematite, goethite and clays and type II: Softer aluminous laterites tending to be whitish or limonitic (yellowish)[2,4]. Both these types of ores are associated with large quantities of clays and quartz. The LGIO fines mostly consist of softer aluminous laterites whitish or limonitic (yellowish) in color and have a high content of clay and quartz material.

Generally, the Fe content is very low. These ores consist of hematite goethite minerals with excessive quartz Al and P as clout in goethite resulting in significant implications on the quality and performance of iron ore used for iron making. Goethite, being softer than hematite, tends to produce fines during comminution[7].

Consequently, it is increasingly important to process hematite-goethite iron ores and fine concentrates to produce sinter and pellet feedstocks of acceptable grade for iron making due to changing ore characteristics[9].

There are several methods available to enhance the quality of low-grade iron ores in the field of mineral processing. These methods depend on physical characteristics such as size, magnetic properties, density and surface chemistry.[1,3,5]

The primary objective of these methods is to eliminate the unwanted gangue materials from the iron-bearing minerals while minimizing impurities, particularly SiO_2, Al_2O_3 and P. The present research work focuses on enriching goethite-rich ores to obtain top-quality concentrates for ironmaking using wet processing techniques such as scrubber, hydro cyclones spirals and HGMS[11,12].

Table 1
Chemical analysis of iron ore sample

Constituent	Wt%
Fe	34.80
SiO_2	22.24
Al_2O_3	12.93
LOI	8.93

The SEM-EDS analysis of low-grade laterite iron ore lumps is shown in Figure 2. This analysis was conducted to determine the morphology and chemical constituents of the ore. Figure 2 shows the uneven distribution of iron ore particles.

Figure 3 shows the EDS spectrum of the iron ore sample in selected area for the presence of different elements. During EDX measurement, different areas were focused for the representative samples of lumps i.e. - 150+75µm, -75+45µm and -45µm. Both Fe and Si can be seen in the EDX spectrum.

In the EDX spectrum, the quantities of Fe, Si and Al are 54.70%, 7.03% and 7.98% respectively. Table 2 gives the elemental distribution of different elements for the selected areas of lumps of different particle size.

https://doi.org/10.25303/185da1770185

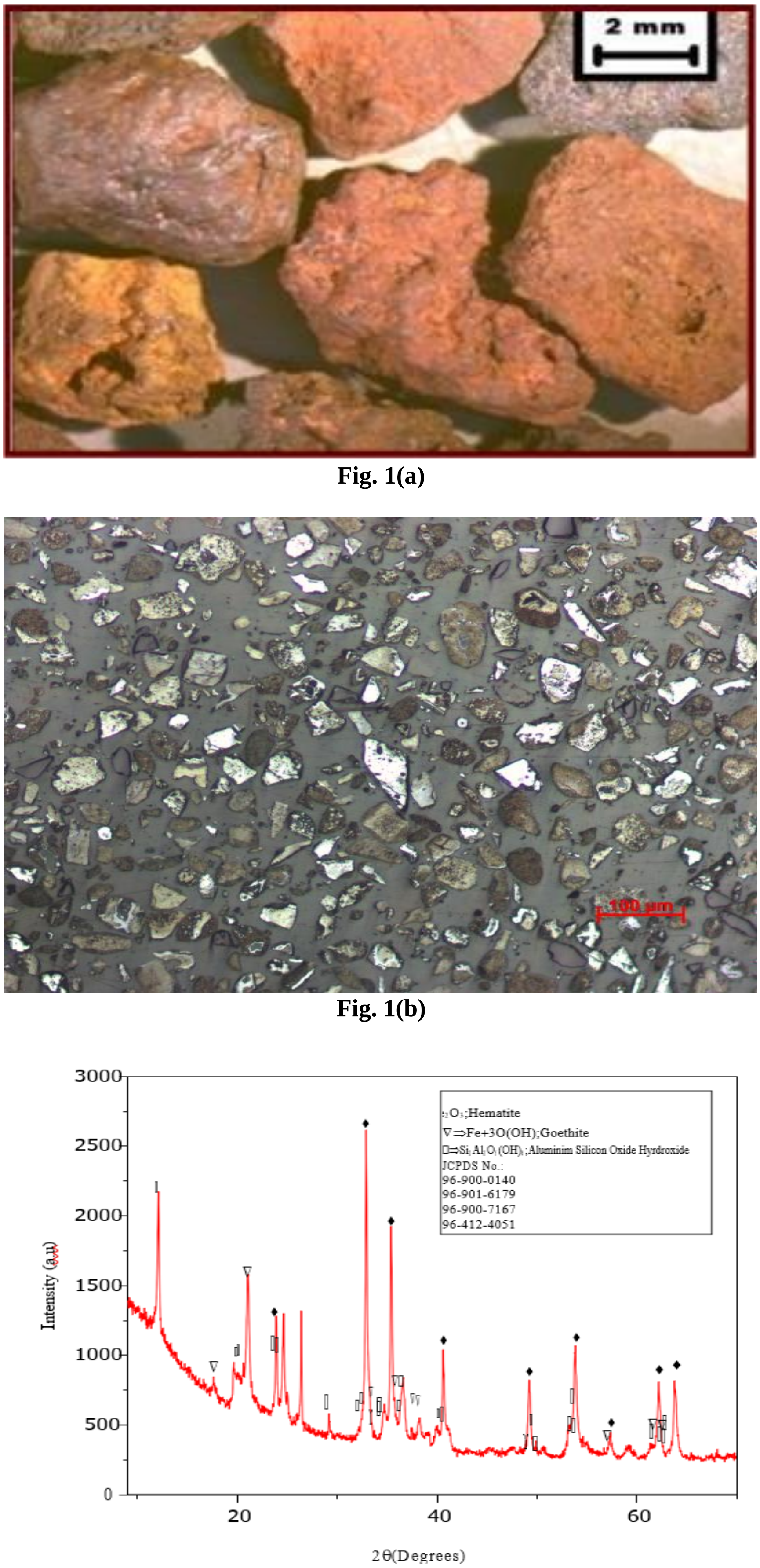

Fig. 1(a)

Fig. 1(b)

Fig. 1(c)

Fig. 1: (a) Hematite body enclaved in the laterite iron ores, (b) optical microscope image for the feed sample and (c) XRD spectra image

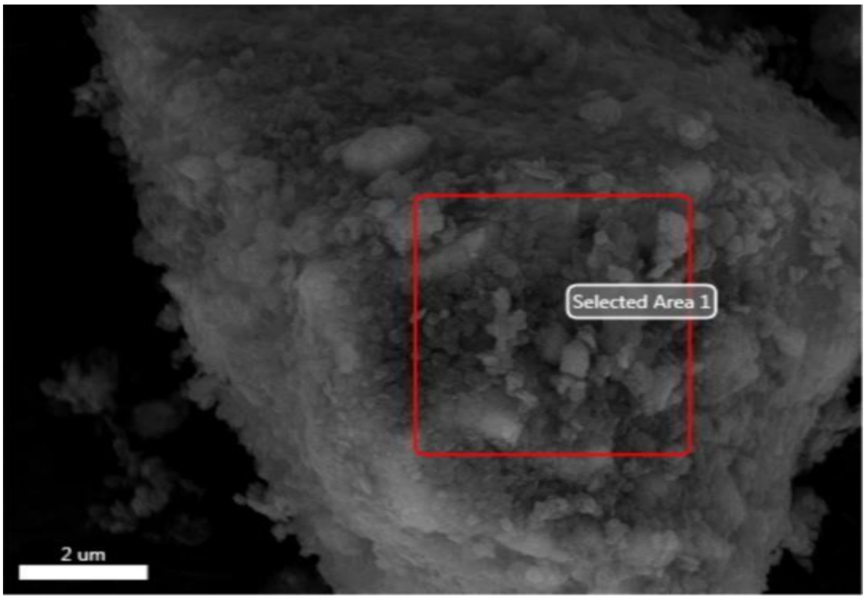

Fig. 2: SEM image of lumps

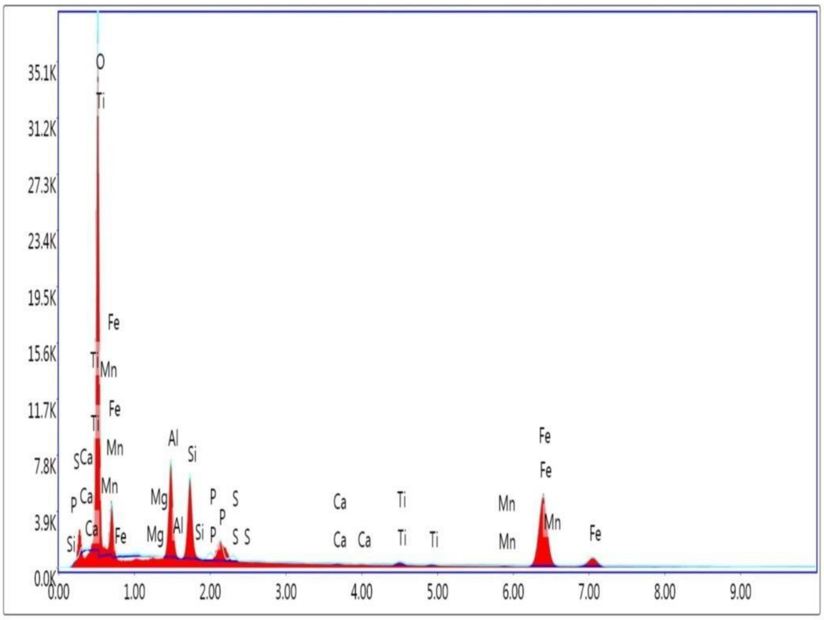

Fig. 3: Area analysis of hematite grains, silica and other elements in laterite iron ore of lumpswith EDS revealing composition distribution of Si, Fe, O

Table 2
Elemental distribution of different elements for the selected areas of lumps ofdifferent particle size

Element	Weight %		
	-150+75µm	-75+45µm	-45µm
O K	27.72	41.85	43.39
Mg K	0.00	0.18	0.16
Al K	7.98	23.94	23.23
Si K	7.03	23.78	22.73
P K	0.59	0.49	0.58
S K	0.56	0.44	0.52
Ca K	0.19	0.16	0.31
Ti K	0.94	1.86	2.72
Mn K	0.30	0.11	0.12
Fe K	54.70	7.17	6.24

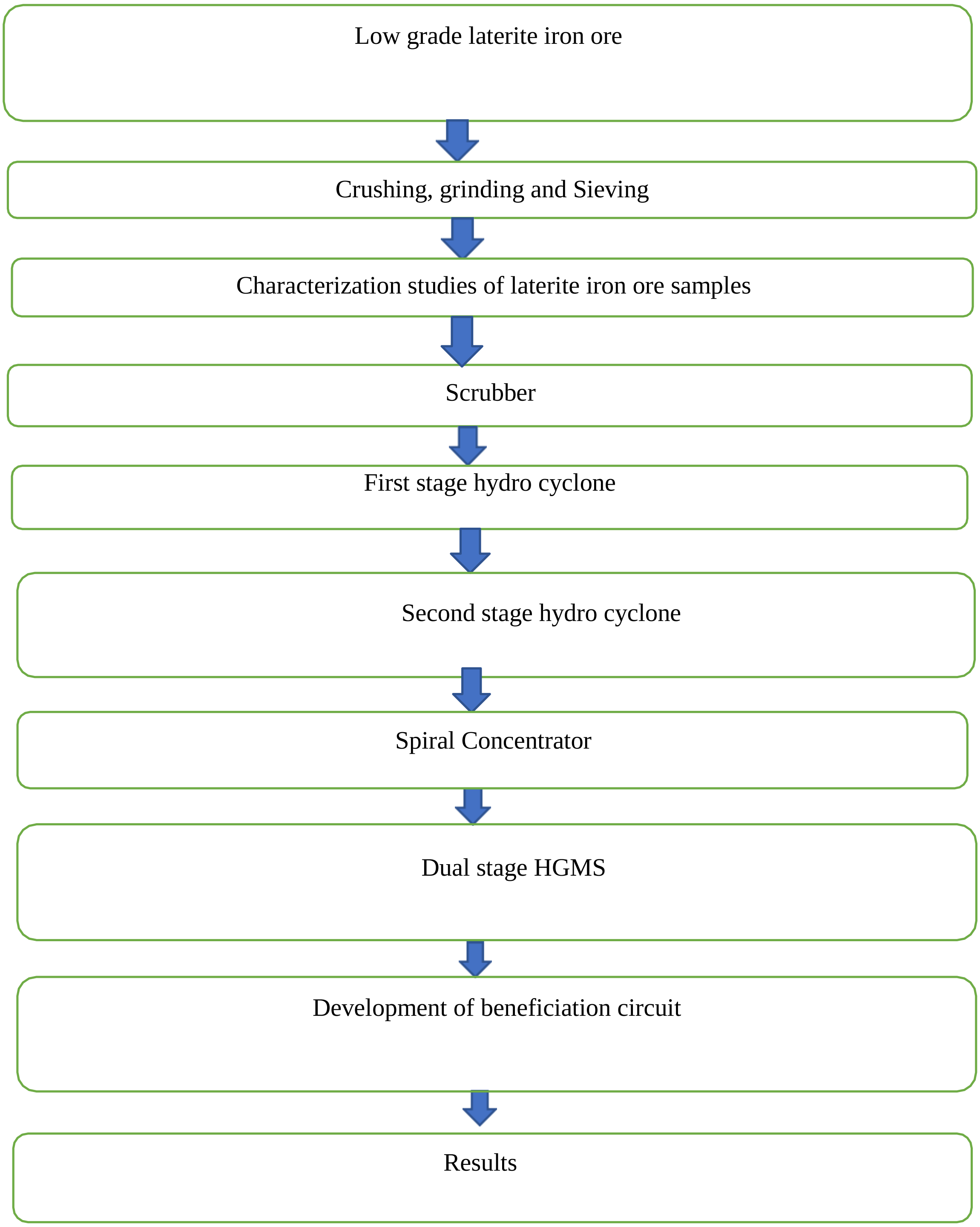

Fig. 4: Experimental flow chart followed for maximum recovery of iron values

Material and Methods

The laterite iron ore sample used in the present study was collected from mines in Gujarat. The photo of the laterite sample and optical microscope in figure 1 (a,b) exhibits the hematite enclaved in laterite ore and the mineralogy complexity of iron minerals with gangue minerals. The XRD image shown in figure 1c represents the hematite, rich in goethite and quartz. The as-received laterite samples were subjected to particle size distribution using standard sieves. The bond work index for the sample is 11.0 kWh/t. Later the ore is crushed using a jaw and roller crusher and ground using a laboratory ball mill. Further, the representation sample was obtained using the coining and quartering method. The experimental flow chart for the maximum recovery of iron values is shown in figure 2.

The experiments were carried out in scrubber, hydro cyclone, spirals, dual stage HGMS, magnetic separator and microwave reduction roasting.

Scrubbing: The scrubbing process was carried out with a variation of independent parameters such as feed rate of 1.5 kg/min, 2.0 kg/min and 2.5 kg/min, rotary speed of 50 rpm, 100rpm and 150rpm and angle of inclination of 10°, 15° and 20°of the scrubber.

Two-stage hydro cyclone: The primary hydro cyclone's overflow and tailings underwent a second stage of separation of cyclone specification size: 4 inches (10.16 cm), vortex finder diameter: 25mm, Spigot diameter: 17mm, standard hydro cyclone of 4-inch diameter supplied by WEIR Minerals, was used for primary and secondary hydro cyclone test work.

Spiral Concentrator: The spiral concentrator supplied by smart systems was used for the experiments. Feed rate: Lightweight 4-way distributor to handle up to 40 gpm slurry, power of 4 pole, 16 Amp MCB (3 Phase + neutral with earthing) AC, 50/60Hz, 415 V Motor 2.25 kW (3 HP), 1415 rpm.

Dual Stage HGMS: The tests were conducted in a pilot scale model SL on vertical ring and pulsating high-gradient magnetic separator with a 1.5 mm grid plate (matrix mesh) at a magnetic intensity of 9000 gauss. The quantitative analysis of iron was carried out using standard titration procedures in the concentrate and tailings. Further, the mineral phase analysis was carried out using X-ray spectrum diffraction (XRD).

Results and Discussion

Scrubbing process: In the present study, the soft and friable lateritic masses, fine sand and limonitic clay particles from iron ore were removed by scrubbing. The feed contains crushed iron ore and water in a 60:40 ratio to the scrubber. The scrubbing operation is carried out on iron ore feed samples of -150 microns. The concentrate product has a Fe content of 37.56% with a weight recovery of 55.6%, while the tailings contain 33.30% Fe with a weight recovery of 44.4%.

Two-stage Hydro cyclone: The concentrate from the scrubber unit is processed in the primary hydro cyclone. The primary cyclone has the following test conditions of cyclone size: 4 inches (10.16 cm), Vortex finder diameter: 40 mm, Spigot diameter: 15 mm, Feed density: 1.11 g/cc, Feed pressure: 1.0 to 1.2 bar, Overflow density: 1.07 g/cc and Underflow density: 1.65 g/cc. The primary hydro cyclone underflow contained 39.4% Fe with 28.63% weight recovery, while the overflow fraction contained 35.68% Fe with 26.96% weight recovery. The chemical analysis of the primary hydro cyclone feed and products is shown in table 4.

The primary hydro cyclone's overflow and tailings underwent a second stage of separation with operating conditions of feed density: 1.07 g/cc, feed pressure: 1.5 to 1.8 bar, overflow density: 1.03 g/cc and underflow density: 1.12 g/cc. The secondary hydro cyclone's underflow contained 38.05% Fe with 24.68% weight recovery, while the overflow had 30.35% Fe with 45.88% weight recovery. The chemical analysis for feed and product is shown in table 5.

Spiral concentrator: In this study, we used a spiral concentrator to increase the iron content further in the underflow from the primary hydro cyclone and secondary cyclone. We tested the concentrator under specific conditions: Feed rate: 4.0 to 4.52 m3/hr, feed density: 1.20 to 1.23 g/cc**,** concentrate density: 2.10 g/cc, tailing density: 1.15 to 1.16 g/cc and spiral tailing density: 1.14 g/cc.

Table 3
Feed and Product analysis of Scrubber

	Wt.%	**Fe (T)**	**SiO_2**	**Al_2O_3**
Feed	100	35.43	22.24	12.96
Concentrate	55.6	37.56	16.58	10.64
Tailing	44.4	33.30	28.59	15.4

Table 4
Feed and Product analysis of Hydro cyclone 1

	Wt.%	**Fe (T)**	**SiO_2**	**Al_2O_3**
Feed	55.6	37.56	16.58	10.64
Concentrate	28.63	39.4	14.38	9.7
Tailing	26.96	35.68	18.79	11.58

Table 5
Feed and products analysis of Secondary hydro cyclone, %

	wt%	**Fe(T)**	**SiO_2**	**Al_2O_3**
Feed	71.4	34.2	24.8	13.94
Over flow	45.88	30.35	26.0	14.44
Under flow	24.68	38.05	23.84	12.04

The concentrate product contains 42.07% Fe with 29.62% weight recovery and the tailing fraction contains 35.28% Fe with 23.68% weight recovery. The chemical analysis and particle size distribution for the spiral concentrator feed and products are shown in table 6.

Dual-stage HGMS: The spiral concentrator tailings were processed using HGMS (High Gradient Magnetic Separator) to recover iron values. The experiments were conducted at the operating test conditions of a feed density of 1.13 g/cc Mag concentrate density: of 1.15 g/cc, non-Mag: 1.08 gm/cc, feed density: of 1.13 gm/cc and a magnetic field intensity of 9000 G. The rougher HGMS yielded a magnetic fraction with 40.89% Fe at 11.96% yield, while the non-magnetic fraction contained 29.67% Fe at 11.72% weight shown in table 7.

The non-magnetic fraction from rougher HGMS was subjected to scavenger HGMS for further upgrading. The operating parameters are: feed density is 1.08 g/cc. Mag concentrate density: 1.10 to 1.11 g/cc. non-Mag: 1.04 to 1.05 g/cc, magnetic field intensity: 10000 Gauss. The magnetic intensity of HGMS was 10000 G. The Fe content of the scavenger HGMS magnetic fraction enhanced to 38.17% Fe with a yield of 6.4% and the non-magnetic fraction has 21.17% Fe with a weight of 5.24%. Scavenger HGMS feed and products chemical analysis are shown in table 8.

Development of Beneficiation Circuits: Figures 5 and 6 show the beneficiation circuits of the laterite ores. The results concluded that the concentrate of 51.12% FeG and recovery of 29.40%Fe_R were obtained, which are not feasible for iron making in blast furnace. From mineralogical studies, shown in figure 4, it was found that the goethite phase has partially reported to the concentrate and maximum alumina and quartzite gangue minerals are associated with the goethite phase leading to a lesser reduction in alumina and silica in the final concentrate.

Table 6
Feed and product analysis of spiral concentrator, %

	Wt.%	Fe(T)	SiO_2	AL_2O_3
Feed	53.31	39.06	18.75	10.8
Concentrate	29.62	42.07	17.84	9.81
Tailing	23.68	35.28	19.89	12.04

Table 7
Feed and product analysis of Primary HGMS, %

	Wt%	Fe(T)	SiO_2	AL_2O_3
Feed	23.68	35.28	19.89	12.04
Mag	11.96	40.89	18.35	9.88
Non-Mag	11.72	29.67	21.43	14.25

Table 8
Feed and product analysis of scavenger HGMS, %

	Wt	Fe(T)	SiO_2	AL_2O_3
Feed	11.72	29.67	21.43	14.25
Mag	6.4	38.17	18.65	10.32
Non-Mag	5.24	21.17	24.8	19.1

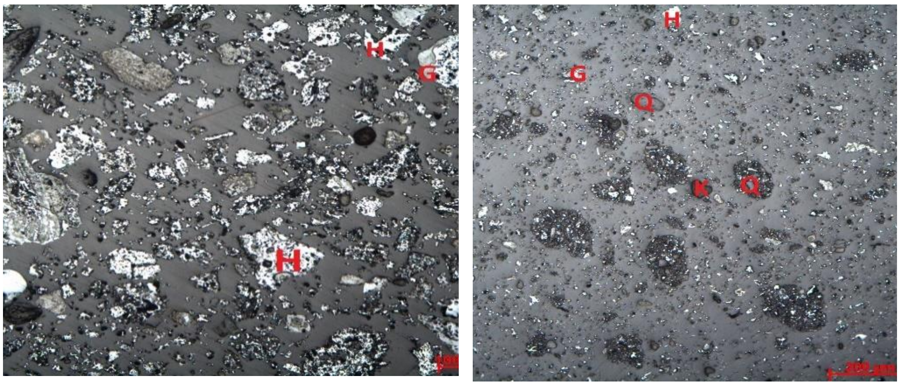

Concentrate **Tailing**

Fig. 5: Optical micrographs of Concentrate and Tailings

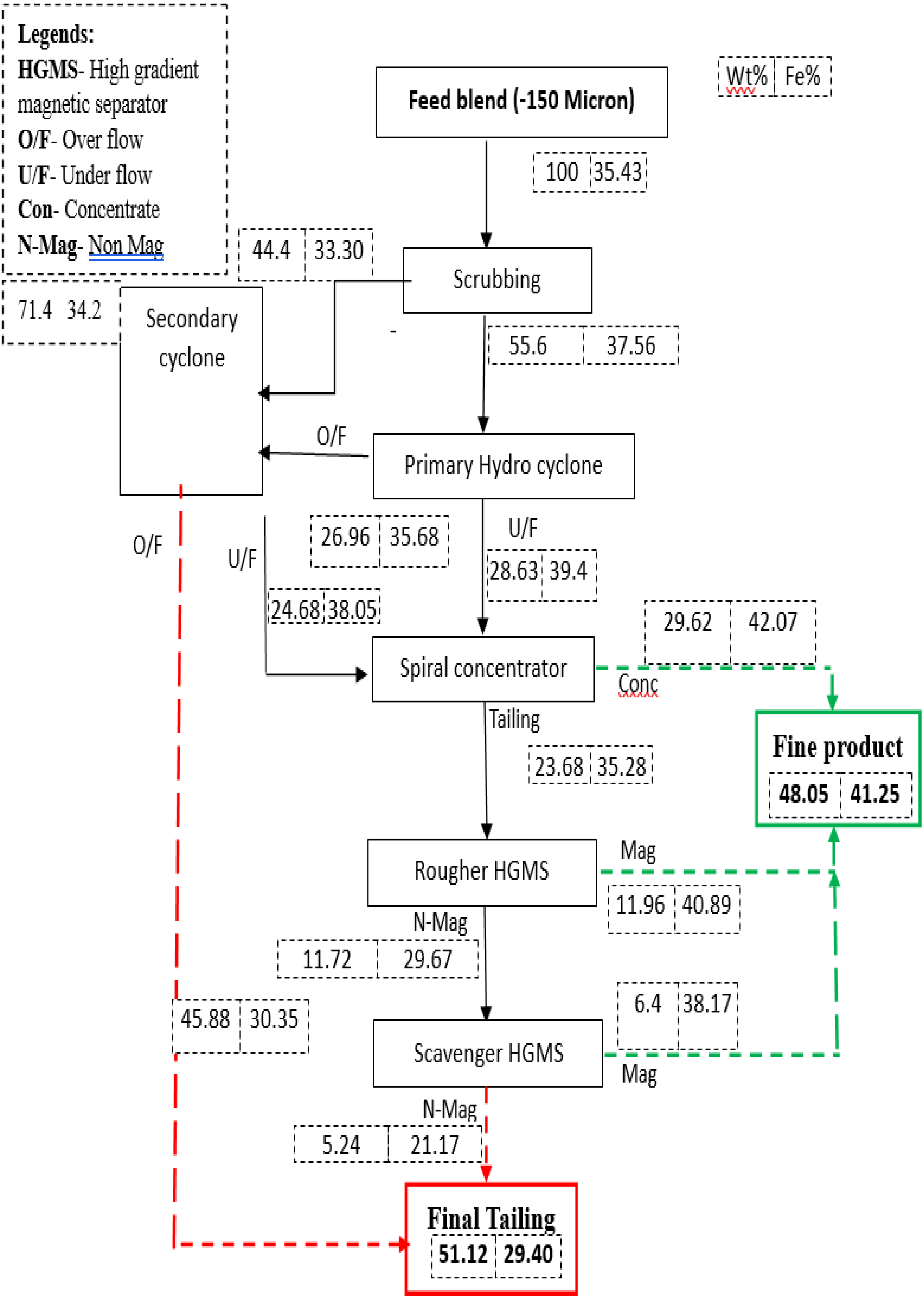

Fig. 6: Process flow sheet – Circuit 1 with mass balance

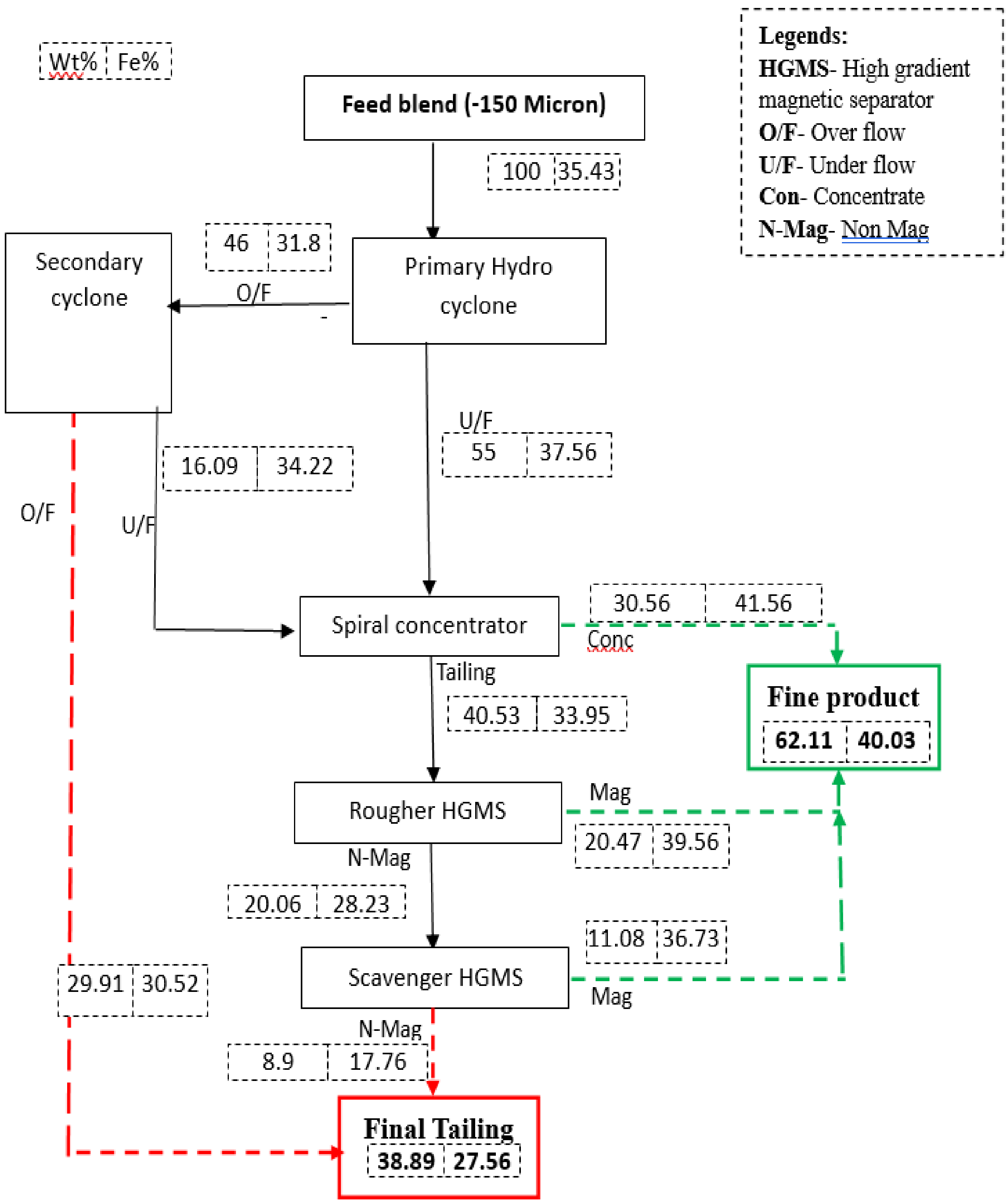

Fig. 7: Process flow sheet – Circuit 2 with mass balance

Conclusion

The two different circuits for beneficiation were tried to optimize the product quality. The final concentrate obtained from pilot scale beneficiation process 1 consists of 41.25 % Fe with 48.04 % weight recovery and the tailing loss is 51.12 % by weight with 29.4 % Fe. The final concentrate obtained from pilot scale beneficiation process 2 consists of 40.03 % Fe with 62.11 % weight recovery and the tailing loss is 38.89 % by weight with 27.56 % Fe.

References

1. Akbari H., Noaparast M., Shafaei S.Z., Hajati A., Aghazadeh S. and Akbari H., A beneficiation study on a low-grade Iron ore by gravity and magnetic separation, *Russ. J. non-Ferr. Met.*, **59**, 353-363 **(2018)**

2. Clout J.M.F. and Manuel J.R., Mineralogical, chemical and physical characteristics of iron ore, Iron ore: Mineralogy, processing and environmental sustainability, ed., Lu L., 45–84 **(2015)**

3. Das B. and Rath S.S., Existing and new processes for beneficiation of Indian Iron Ores, *Trans. Indian Inst. Metals*, **73(3)**, 505-514 **(2020)**

4. Davis C. Yang, In Reagents in Mineral Processing, Somasundaran P. and Moudgil B.M., eds., Marcel Dekker Inc., New York, USA, 585 **(1987)**

5. Dey S., Mohanta M.K. and Singh R., Mineralogy and textural impact on beneficiation of goethitic ore, *Int. J. Min. Sci. Technol.*, **27**, 445-450 **(2017)**

6. Indian Minerals Year Book, Indian Bureau of Mines, Nagpur, **20076**, 47-1 **(2006)**

7. Manuel J.R. and Clout J.M.F., Goethite, classification, distribution and properties with reference to Australian iron ore deposits, Proceedings Iron Ore, Australasian Institute of Mining and Metallurgy, Melbourne, 567–74 **(2017)**

8. Mohanraj G.T., Rahman M.R., Joladarashi S., Hanumanthappa H., Shanmugam B.K., Vardhan H. and Rabbani S.A., Design and fabrication of optimized magnetic roller for permanent roll magnetic separator (PRMS): Finite element method magnetics (FEMM) approach, *Advanced Powder Technology*, **32(2)**, 546-564 **(2021)**

9. O'Conner M. and MacHunter R.M.G., A review of current iron ore processing practices for −8 mm material, Proceedings Workshop on Iron Ore Beneficiation, Indian Institute of Metals, Jamshedpur, 1–5 **(2006)**

10. Richards R.G., MacHunter D.M., Gates P.J. and Palmer M.K., Gravit separation of ultra-fine (−0.1mm) minerals using spiral separators, *Miner. Eng.*, **13**, 65-77 **(2000)**

11. Santosh, T., Angadi S.I., Dash N., Eswaraiah C. and Tripathy S.K., Characterization and Comminution studies of Indian low grade iron ores, *Mining, Metallurgy & Exploration*, **36**, 303-312 **(2019)**

12. Seifelnassr A.A.S., Moslim E.M. and Abouzeid A.Z.M., Effective processing of low-grade iron ore through gravity and magnetic separation techniques, *Physicochem. Probl. Miner. Process*., **48**, 567-578 **(2012)**

13. SME Handbook of Mineral Processing, Weiss N.L., ed., SME/ AIME Publication, New York, USA, 20-2 **(1985)**

14. Wang Chaohui, Environmental effects and enhancement mechanism of graphene/tourmaline composites, *Journal of Cleaner Production*, **262**, 121313 **(2020)**.

(Received 22nd January 2025, accepted 20th February 2025)